Systems pharmacology of the amyloid cascade : unfolding oligomer modulation in Alzheimer's disease

Maanen, E.M.T. van

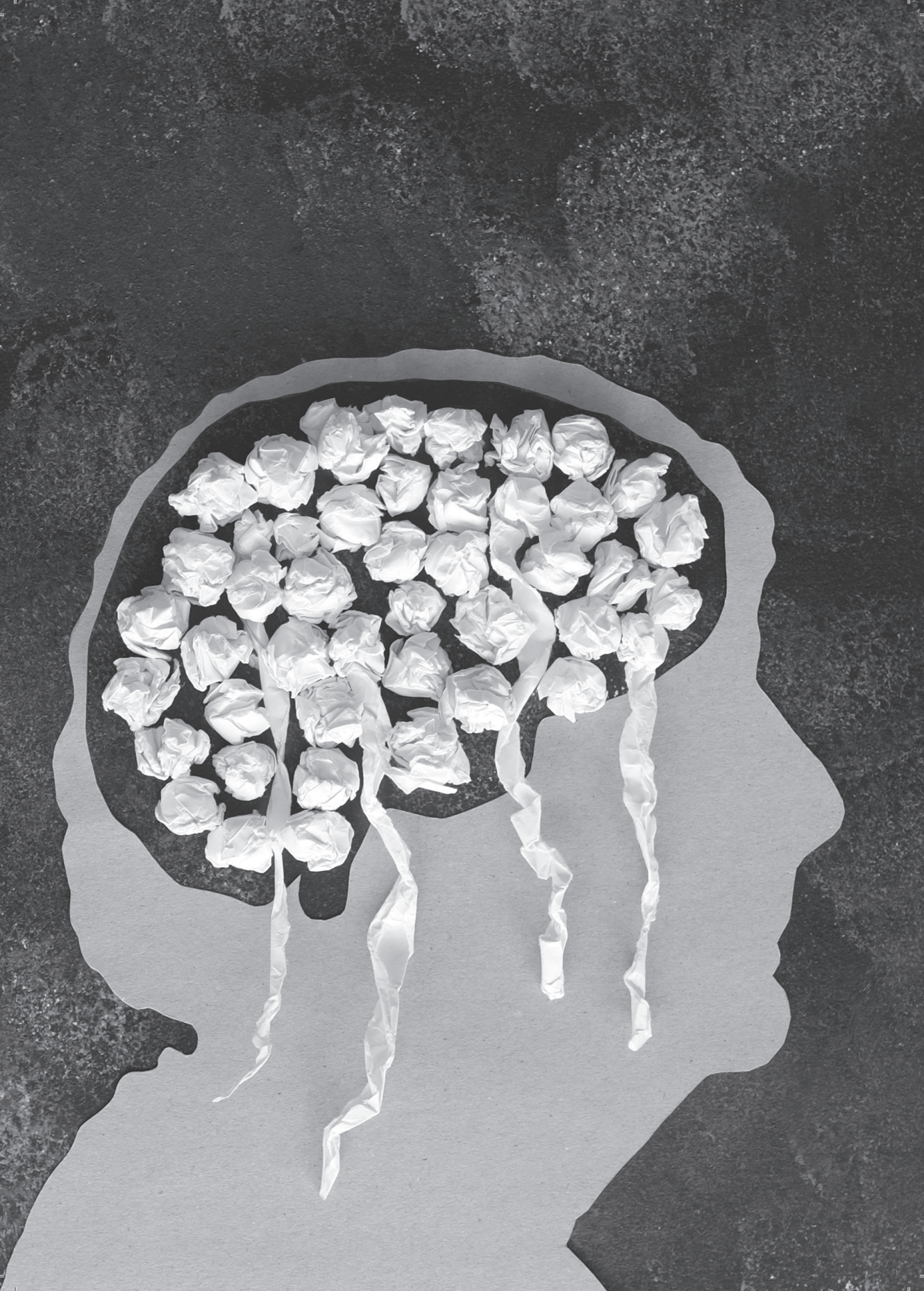

Section IV

Systems pharmacology of the amyloid cascade

Summary, conclusions & perspectives

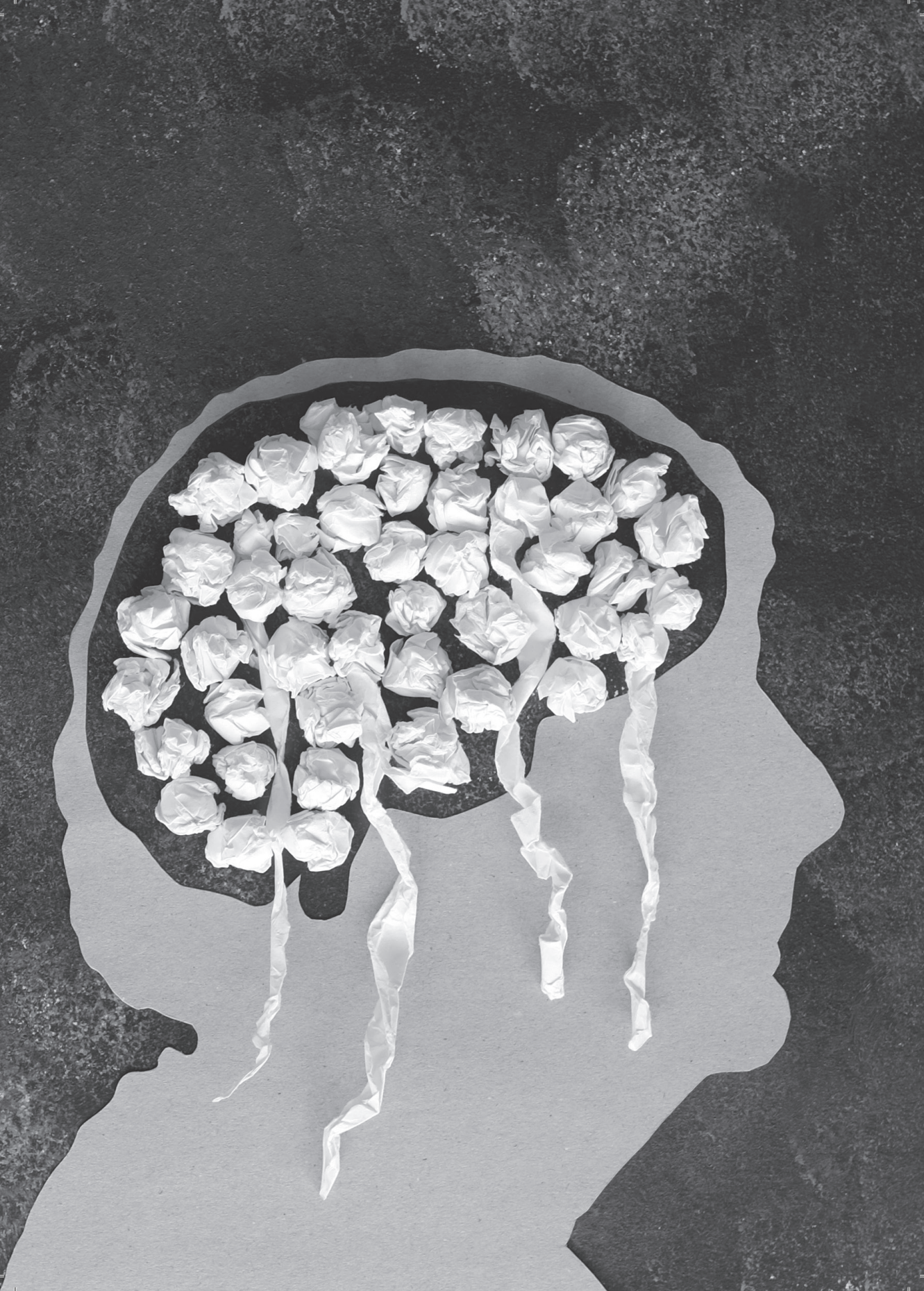

Chapter 8

Systems pharmacology of the amyloid precursor protein pathway in Alzheimer's disease

Conclusions & perspectives

Introduction and objectives

The leading cause of cellular dysfunction in neurodegenerative diseases is the accumulation of protein aggregates inside or outside of neurons. These aggregates are phenotypically different but biochemically similar across neurodegenerative diseases suggesting a conserved molecular mechanism of pathogenesis. This is consistent with the observation that neurodegenerative disorders as Alzheimer's disease (AD), Parkinson's disease (PD), Huntington's disease (HD) and motor disorders such as amyotrophic lateral sclerosis (ALS) present the same pattern of progression of neuronal death, nervous system deterioration and cognitive impairment. Presumably these pathological changes are driven by an error in protein conformation followed by abnormal aggregation to form pathogenic assemblies ranging from small oligomers to large amyloid masses. The amyloid cascade hypothesis of AD provides a framework for protein misfolding neurodegenerative diseases.

AD is presently incurable, as the loss of neurons is irreversible and none of the currently available treatments attenuates the progression of the pathological cascade. According to the amyloid hypothesis, proteolytic processing of amyloid precursor protein (APP) to form the amyloid-beta (Aβ) peptides plays a central role in the pathophysiology of AD. Aβ levels are increased early in the disease process, forming toxic soluble Aβ oligomers (Aβ_{O}) and plaques. Aβ_{O} are considered to be a primary driver of the neurodegeneration in AD brain. In the APP processing and clearance pathways, APP is cleaved sequentially by β-secretase (BACE1) and γ-secretase (GS) to produce Aβ.

The drug effects on the individual attributes of the APP pathway are difficult to predict, because of the complexity of the underlying biochemical network that governs the formation and elimination of the individual components. As a consequence also, the effect on Aβ_{O}s and on the Aβ equilibrium after inhibiting Aβ production or enhancing Aβ clearance is largely unknown. A systems pharmacology modelling approach, describing the interactions in the underlying biochemical network, will provide a mechanistic understanding of the behaviour of the APP pathway, enabling the prediction of therapeutic effects on Aβ and indirectly also on Aβ_{O} concentrations (**Chapter 2**).

The objectives of the investigations described in this thesis were: (1) To establish a systems pharmacology model to describe in a strictly quantitative manner the biochemical network of APP processing; (2) to predict and evaluate the effect of Aβ production inhibitors, acting at different sequences in the APP processing pathway, on Aβ_{O} concentrations; (3) to explore other therapeutic strategies which may aid the reduction of

Aβ_O burden.

Development of a systems pharmacology model to predict the oligomer response following secretase inhibition

The effects of Aβ production inhibitors were characterized in conscious cisterna-magna-ported (CMP) rhesus monkeys. In these CMP rhesus monkeys a permanent catheter was implanted into the cisterna-magna enabling repeated sampling of cerebrospinal fluid (CSF) collection in conscious monkeys (Figure 8.1)[1]. With this animal model, detailed studies on the pharmacokinetics (PK) and pharmacodynamics (PD) of potential APP modifying drugs in the central nervous system can be performed, which is difficult to achieve in humans.

Table 8.1: Summary overview model structures

Model	Inhibitors	Included biomarkers	Chapter
β-APP model	BACE1i (MBi-5)	sAPPβ, sAPPα, Aβ40, Aβ42	3
β-13C-APP model	BACE1i (MBi-5)	sAPPβ, sAPPα, Aβ40, Aβ42, **fraction labeled Aβ, fraction labeled sAPPα, fraction labeled sAPPβ**	4
β-γ-APP model	BACE1i (MBi-5) **GSi (MK-0752)**	sAPPβ, sAPPα, Aβ40, Aβ42 **Aβ40, Aβ42**	5
β-O-APP model	BACE1i (MBi-5)	sAPPβ, sAPPα, Aβ40, Aβ42, **Aβ38, Aβ_O**	6
β-γ-O-APP model	BACE1i (MBi-5) GSi (MK-0752)	sAPPβ, sAPPα, Aβ40, Aβ42, Aβ38, Aβ_O **sAPPβ, sAPPα**, Aβ40, Aβ42, **Aβ38, Aβ_O**	7

In a series of investigations, we have developed a systems pharmacology model for the APP processing pathway. The various steps in the development of this model are summarized in Table 8.1 and presented in Figure 8.2-Figure 8.6. First, we established a systems pharmacology model of the APP processing pathway to characterize the influence of BACE1 inhibition on the concentrations of the APP metabolites sAPPβ, sAPPα, Aβ40, Aβ42 (Figure 8.2) (**Chapter 3**). In this so called β-APP model, the effect of the BACE1 inhibitor MBi-5 was described by inhibition of the formation of sAPPβ out of APP, where sAPPβ was used as surrogate of C99, to drive the Aβ formation. This analysis showed that upon BACE1 inhibition the concentration of the metabolite sAPPα increased

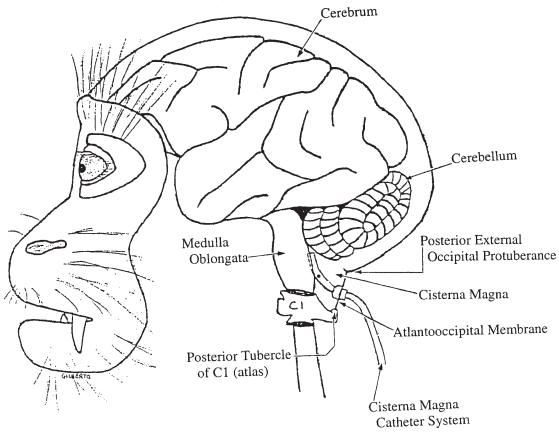

Figure 8.1: Schematic of lateral view of implant placement in rhesus monkey head.
The rhesus monkeys were surgically implemented with a catheter system which was placed 1.0 cm into the cisterna, facilitating direct access to CSF outflow from the cisterna magna. The catheter was attached to a titanium port placed subcutaneously between the shoulder blades to allow easy access for sampling CSF in a conscious, chaired rhesus monkey. Figure from Gilberto et al. [1].

and while the concentrations of the metabolites Aβ40, Aβ42 and sAPPβ decreased in a dose-proportional manner. Analysis of the changes in the monomeric Aβ species with the β-APP model enabled prediction of a reduction of the putative neurotoxic Aβ_{O} pool. Also, the findings indicated that decreases in monomeric Aβ responses resulting from BACE1 inhibition were partially compensated for by dissociation of Aβ_{O}.

The next step in the model development was the interfacing of the β-APP model with tracer kinetic data obtained with the so-called stable-isotope-labeling kinetics (SILK) protocol (**Chapter 4**). The SILK protocol was originally used to quantify differences in the Aβ kinetics between patients with AD and their cognitively normal controls. Here the SILK protocol was applied for the first time to examine the effect of BACE1 inhibition on the fraction labelled Aβ, fraction labelled sAPPα and fraction labelled sAPPβ after $^{13}C_6$-Leucine infusion, which was started at 1 hour after the administration of MBi-5. Interfacing of the tracer kinetic data with the β-APP model yielded the next version of the systems pharmacology model of the APP pathway, the β-13C-APP model (Figure 8.3).

The β-13C-APP model distinguished labelled and unlabelled species and also separated steps in the biotransformation and the distribution of APP peptides to CSF. This improved the understanding of the dose-proportionality of the effect on the fraction labelled sAPPβ and the lack of such a dose-proportional response in fraction labelled

sAPPα. A disconnect between Aβ response measurements that were obtained with the data from the enzyme-linked immunosorbent assay (ELISA) and SILK was found, that may be explained by on the one hand the formation of an unknown APP fragment with differing kinetics or, on the other hand an unknown process that influenced the result of the SILK assay. In the modelling this effect was accounted for by inclusion of the model component FactorX.

A limitation of the β-APP model was that the influence of γ-secretase cleavage step could not be separated from an effect on sAPPβ elimination. Therefore, in **Chapter 5** the β-APP model was extended to describe Aβ40 and Aβ42 response to GS inhibition. This led to the third version of the model, the β-γ-APP model, which contains separate descriptions to characterize the sequential cleavage steps of APP by BACE1 and GS while the elimination of sAPPβ is described by a separate parameter (Figure 8.4). The β-γ-APP model was identified on the basis of a simultaneous analysis of APP metabolite response data following the administration of the BACE1 inhibitor MBi-5 (1 study; effects on the metabolites Aβ40, Aβ42, sAPPβ and sAPPα) and the GS inhibitor MK-0752 (2 studies; effects on Aβ40 and Aβ42), respectively. This analysis revealed a difference in Aβ dynamics after BACE1 versus GS inhibition, which was reflected in a different value of the Aβ40 formation rate constant. Further, the model based prediction of Aβ_{O} suggested a lower oligomerization rate of Aβ42 after GS then after BACE1 inhibition. Unfortunately, in this investigation, the identified differences in Aβ dynamics after BACE1 or GS inhibition could not be separated from study differences, as levels of CSF biomarkers can vary between studies *(vide infra)*.

Application of the systems pharmacology model to characterize oligomer modulation following secretase inhibition

In the previous studies we have obtained indirect information on the formation of Aβ_{O}, through the analysis of the effects of secretase inhibitors on the monomeric species. This was necessary, because no direct measurements of the Aβ_{O} were available. In this respect it should be realized that it is extremely difficult to measure the low concentrations of the Aβ species[2,3]. In the meantime however an assay had become available for direct measurement of Aβ_{O}[4]. It was therefore of great interest to compare the model based prediction of Aβ_{O} response to BACE1 and GS inhibition with the observed Aβ_{O} response measurements. In the fourth study therefore the effects of MBi-5 and MK-0752 on the CSF concentrations of five APP metabolites (sAPPβ, sAPPα, Aβ40, Aβ42, Aβ38)

and Aβ_O were determined. The study was designed in a 4-way full crossover design. The APP systems model was extended to describe the effect of BACE1 inhibition on an additional Aβ isoform (Aβ38) and to capture Aβ_O response measurements (**Chapter 6**; β-O-APP model). The model was advanced further to describe GS inhibitor response data (sAPPβ, sAPPα, Aβ40, Aβ42, Aβ38, Aβ_O), which ultimately led to the β-γ-O-APP model (**Chapter 7**).

Before analysing the data on the basis of the β-O-APP model, a subset of the data (the effects on the peptides sAPPβ, sAPPα, Aβ40 and Aβ42) was analysed on the basis of the original β-APP model. This was necessary, because due to changes in the sample pre-treatment and the analytical methodology the absolute values of the concentrations in these studies differed from those in previous investigations, leading to different values of the model parameters. Using a within-study comparison, it was shown that the onset and maximum observed Aβ_O response was underpredicted by the β-APP model. As a next step therefore, the monomeric Aβ (Aβ38, Aβ40, Aβ42) and Aβ_O response measurements were incorporated in the fourth version of the model (Figure 8.5). This analysis showed that the Aβ oligomerization follows second order kinetics. Furthermore, the model also provided evidence that dissociation of Aβ_O, restoring the balance with Aβ monomers (homeostatic adaptation), contributes to the ultimate treatment effect. This analysis also showed that, of the various peptides, Aβ42 is the main monomeric Aβ species that drives the Aβ oligomerization, which is in line with the general belief that Aβ42 is the Aβ species prone to toxic aggregation.

In **Chapter 7**, the β-O-APP model was extended to simultaneously describe the effect of BACE1 and GS inhibition and to capture Aβ_O response data to inhibitors of both enzymes (Figure 8.6). In the β-γ-O-APP model the sequential cleavage steps by BACE1 and GS were described separately, in a manner that is similar to the β-γ-APP model. With this analysis, information on the sAPPβ, sAPPα, Aβ38, and Aβ_O response to GS inhibition was included. Quite unexpectedly, this revealed that upstream of the GS cleavage step in the APP pathway, changes in sAPPβ and sAPPα concentrations in response to GS inhibition were present. The systems analysis of the decrease of sAPPβ and the increase of sAPPα in response to GS inhibition revealed a homeostatic feedback loop regulated via C99: the increase in C99 following GS inhibition stimulated α-secretase processing of APP.

A difference in the ratio Aβ42:Aβ40:Aβ38 between BACE1 versus GS inhibition was found, which was explained by stepwise successive cleavage of C99 by GS, wherein part of Aβ38 is converted from Aβ42. Further, due to the cross-over study design using both

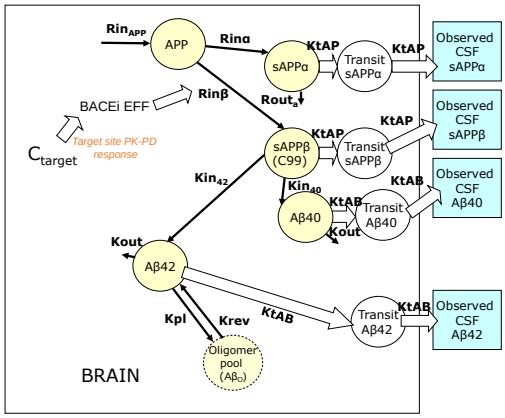

Figure 8.2: *β-APP model (Chpt. 3).* The model comprised nine compartments: Five biomarker compartments in brain *(yellow circles)* and four transit compartments from brain to CSF *(white circles)*. Four biomarkers were measured in CSF (sAPPα, sAPPβ, Aβ40 and Aβ42), indicated by the blue boxes. The model included an Aβ_O compartment *(dashed circle)*. The drug effect of the BACE1 inhibitor *(EFF)* inhibited *Rinβ*. sAPPβ was used in the model structure as a surrogate substrate of C99 in the γ-secretase cleavage step.

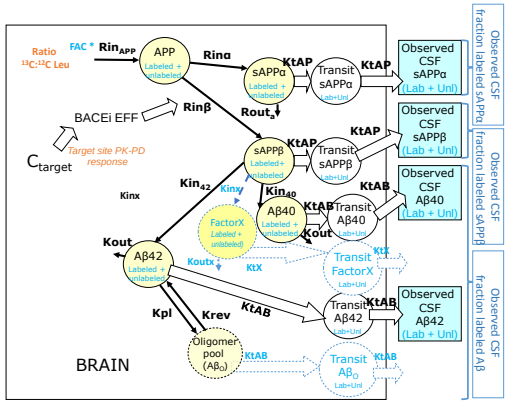

Figure 8.3: *β-13C-APP model (Chpt. 4).* The model comprised two times thirteen compartments: Six biomarker compartments in brain *(yellow circles)*, one oligomer compartment and six transit compartments from brain to CSF *(white circles)*, wherein each compartment was duplicated to track labeled and unlabeled species. Seven biomarkers were measured in CSF (sAPPα, sAPPβ, Aβ40 and Aβ42 (ELISA); fraction labeled sAPPα, fraction labeled sAPPβ and fraction labeled total Aβ (SILK)).The drug effect *(EFF)* inhibited *Rinβ*. sAPPβ was used in the model structure as a surrogate substrate for C99 in the γ-secretase cleavage step. The tracer PK model of label enrichment of the Leucine pool informed label incorporation into the APP pathway. Model extensions compared to the β-APP model are indicated in blue.

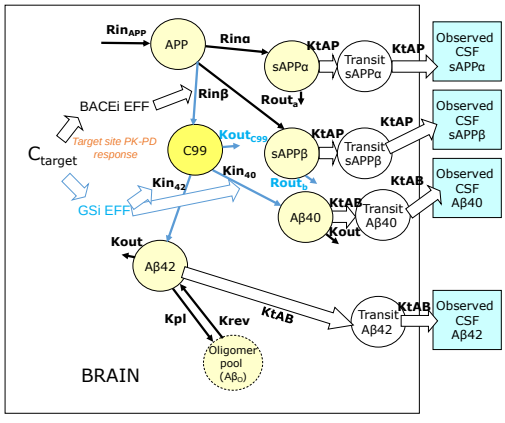

Figure 8.4: *β-γ-APP model (Chpt. 5).* The model comprised eleven compartments: Six biomarker compartments in brain *(yellow)*, one oligomer pool *(blank dashed)* and four transit compartments from brain to CSF *(blank)*. Four biomarkers were measured in CSF (sAPPα, sAPPβ, Aβ40 and Aβ42), indicated by the blue boxes. The model included a C99 compartment, which was not present in the β-APP model. Model extensions compared to the β-APP model are indicated in blue. The drug effect of the BACE1 inhibitor *(BACEi EFF)* inhibited *Rinβ*. The drug effect of the GS inhibitor *(GSi EFF)* inhibited Kin_{42} *and* Kin_{40}.

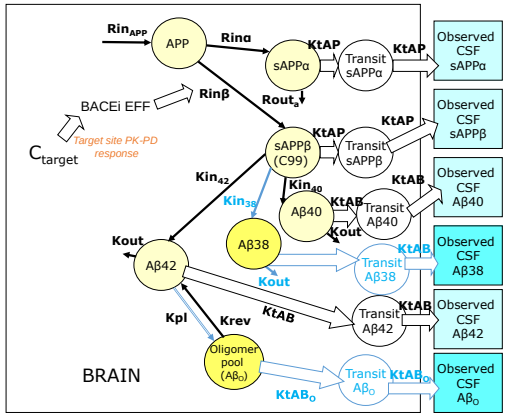

Figure 8.5: *β-O-APP model (Chpt. 6).* The model comprised thirteen compartments: Seven biomarker compartments in brain *(yellow circles)* and six transit compartments from brain to CSF *(white circles)*. Six biomarkers were measured in CSF (sAPPα, sAPPβ, Aβ40, Aβ42, Aβ38 and Aβ_O), indicated by the blue boxes. The drug effect of the BACE1 inhibitor *(EFF)* inhibited *Rinβ*. sAPPβ was used in the model structure as a surrogate substrate for C99 in the γ-secretase cleavage step. Model extensions compared to the β-APP model are indicated in blue.

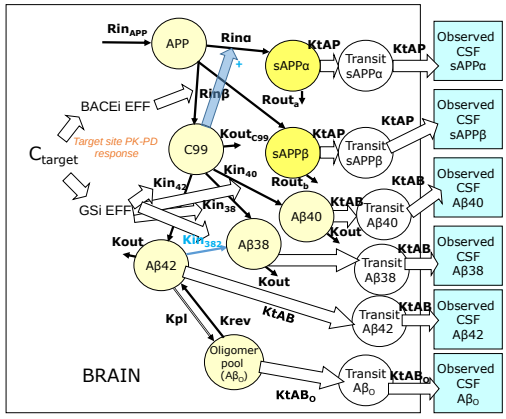

Figure 8.6: *β-γ-O-APP model (Chpt. 7.* The model comprised fourteen compartments: Eight biomarker compartments in brain *(yellow circles)* and six transit compartments from brain to CSF *(white circles)*. Six biomarkers were measured in CSF (sAPPα, sAPPβ, Aβ40, Aβ42, Aβ38 and Aβ_O), indicated by the blue boxes. The drug effect of the BACE1 inhibitor *(BACEi EFF)* inhibited *Rinβ*. The drug effect of the GS inhibitor *(GSi EFF)* inhibited *Kin$_{40}$*, *Kin$_{40}$*, *Kin$_{38}$* and *Kin$_{382}$*. The tick blue arrow indicates the homeostatic feedback on α-secretase through the action of C99. Model extensions compared to the β-O-APP model are indicated in blue.

Figure 8.2 - Figure 8.6:

Advancement of the systems pharmacology model in a series of models (β-APP model (Figure 8.2), β-13C-APP model (Figure 8.3), β-γ-APP model (Figure 8.4), β-O-APP model (Figure 8.5), β-γ-O-APP model (Figure 8.6) to characterize drug effects on the APP pathway. As driver of biomarker responses C_{target} was used in all models, which was derived from the PK models of the BACE1 inhibitor and GS inhibitor, respectively.

APP: Aβ -precursor protein; *Aβ* : amyloid-β-peptide; C_{target}: drug concentration target site; *Kin$_{38}$*: Aβ38 formation rate from C99; *Kin$_{382}$*: Aβ38 formation rate from Aβ42; *Kin$_{40}$*: Aβ40 formation rate; *Kin$_{42}$*: Aβ 42 formation rate; *Kin$_{\text{x}}$*: FactorX formation rate; *Kout*: Aβ38, Aβ40 and Aβ42 degradation rate; *Kout$_{\text{C99}}$*: C99 degradation rate; *Koutx*: FactorX degradation rate; *Krev*: Oligomer dissociation rate; *KtAP*: transit rate sAPPα and sAPPβ from brain to CSF; *Kpl*: Oligomerization rate; *KtAβ* : transit rate Aβ from brain to CSF; *KtAβ $_O$*: transit rate Aβ_O from brain to CSF; *KtX*: transit rate FactorX from brain to CSF; *RinAPP*: source of APP; *Rinβ*: sAPPβ formation rate; *Rinα*: sAPPα formation rate; *Routb*: sAPPβ degradation rate; *Routa*: sAPPα degradation rate.

inhibitors, variation between studies could be accounted for, revealing the true differences in the systems behaviour. Identical values of the systems parameters after BACE1 versus GS inhibition were obtained. Specifically, the lower value of the oligomerization rate constant after GS inhibition that had been observed after the analysis on the basis of the β-γ-APP model could now be explained by the fact that that model did not account for stepwise successive cleavage of C99 by GS.

Identical values of the system specific parameters were observed for the two different interventions (BACE1 versus GS inhibition). This confirms that a true system specific model characterizing the interactions in the APP biochemical network has been obtained. The structure of the final systems pharmacology model of the APP pathway, the so called β-γ-O-APP model, is depicted in Figure 8.6.

In conclusion, a systems pharmacology model of APP processing has been developed which constitutes a basis for the prediction of the influence of therapeutic interventions on the exposure to Aβ_{O}. The systems pharmacology model is based on a network structure. Specific features of the model are i) the Aβ_{O} formation is a second-order process, ii) the treatment effect is influenced by Aβ_{O} dissociation restoring the equilibrium with Aβ monomers and iii) GS inhibition can trigger a homeostatic feedback mechanism promoting the non-amyloidogenic pathway.

Extrapolation of the systems APP model from rhesus monkeys to humans – some preliminary results

An important question is how the model of the APP pathway in monkeys could be adapted to predict, in a quantitative manner the effects of drugs targeting the APP pathway in humans. Here we present some preliminary results of the interspecies scaling of BACE1 inhibition between rhesus monkeys and humans. In this context, first the APP pathway homology of rhesus monkeys to humans is discussed. Next, the considerations in the interspecies translation of drug effects in the β-γ-O-APP model are outlined. Finally, the systems APP model is used to predict CSF response data in humans after BACE1 inhibition.

APP is highly conserved between humans and rhesus monkeys[5]. The 695 amino acid isoform of APP (APP$_{695}$) is completely homologous between humans and rhesus monkeys, whereas the common longer isoform APP$_{770}$ differs in only four amino acids[6]. APP is quite exceptional in having across mammals a totally conserved length and a very high degree of interspecies sequence identity, indicating that the proteolytic processing is

important for the physiological APP function[7]. BACE1, GS and α-secretase sequences are also highly similar between humans and rhesus monkeys with respectively a 99%, 97% and 99% match in amino acids (NCBI homoloGene). Quantitative ELISAs have shown that the concentrations of cerebral Aβ are comparable in patients with AD and aged rhesus monkeys[8]. However, binding assays with radiolabelled Pittsburgh Compound B have shown significant differences in the ligand affinity for Aβ rich cortical extracts from aged nonhuman primates compared to patients with AD. This may be explained by differences in the Aβ aggregates or endogenous cofactors[6]. With the selective Aβ oligomer ELISA assay that was used in the current rhesus studies, oligomers could also be quantified in human CSF[4].

The β-γ-O-APP model consists of eight linked turnover equations for APP, C99, sAPPα, sAPPβ, Aβ38, Aβ40, Aβ42 and Aβ_{O}. The values of physiological turnover rate constants in species other than rhesus monkeys can in principle be predicted based on allometric scaling principles[9]. Therefore, allometric scaling principles were applied to scale the values of the first order rate constants ***Rin***β and ***Rin***α from rhesus monkeys to humans on the basis of body weight using the allometric exponent of -0.25 (Eq. 8.1)[10]. The baseline values of APP, C99, sAPPα, sAPPβ, Aβ38, Aβ40, Aβ42 and Aβ_{O} are considered species independent and were therefore not scaled. The feedback parameter (FP) was dependent on the baseline C99, which is the same in both species. Therefore, FP was also not scaled. This means that intrinsically the values of the zero-order production rate of APP are scaled (Eq. 8.2 and 8.3).

$$R_{human} = R_{rhesus} \cdot \left(\frac{BW_{human}}{BW_{rhesus}} \right)^{-0.25} \tag{8.1}$$

$$\frac{d}{dt} APP = Rin_{APP} - \left(Rin\beta + Rin\alpha \times \left(\frac{C99}{C99_{base}} \right)^{FP} \right) \times APP \tag{8.2}$$

$$Rin_{APP} = (Rin_{\alpha} + Rin_{\beta}) * APP_{base} \tag{8.3}$$

Because of the linkage of the turnover equations in the model, other parameters of the model (***Rout***$_a$, ***Rout***$_b$, ***Kin***$_{40}$, ***Kin***$_{42}$, ***Kin***$_{38}$, ***Kin***$_{382}$, ***Kout***$_{99}$, ***Kout***, ***Kpl***, ***Krev***) are also intrinsically scaled. However, due the linkage of the turnover equations and derived

parameters, the allometric scaling of the system of equations is cancelled out and the values of the system parameters remain unchanged. For the herein reported prediction of APP metabolite responses in human, the values of the system parameters were therefore kept the same as established in rhesus monkey.

Another factor that needs to be taken into account in the scaling is the fact that in the rhesus monkey CSF samples were taken from the cisterna magna, whereas in humans CSF is obtained by a lumbar puncture. A transit compartment model, consisting of a series of transit compartments, was included to account for the delay between the cisterna magna and lumbar CSF biomarker responses, in manner that is similar as previously reported by Kleijn et al. [11]. Thus to translate the β-γ-O-APP model from rhesus monkey to human the following assumptions were made:

(1) APP processing pathway is identical in humans and rhesus monkeys. It is assumed that the identified homeostatic feedback mechanism applies also in humans.

(2) Values of the system parameters are the same in rhesus monkeys and humans.

(3) Values of the drug effect parameters (Imax, IC50) are similar across species.

(4) The delay between the cisterna magna and lumbar CSF biomarker responses can be described by a series of transit compartments.

To evaluate if the β-γ-O-APP model can be translated from rhesus monkeys to humans, with the above mentioned assumptions, the human predictions for the BACE1 inhibitor verubecestat (MK8931) were compared to experimentally determined values that had been reported in the literature [12]. The population PK parameters of verubecestat [13] and reported IC50 in healthy subjects [12] were used to predict the response of the APP metabolites (Aβ40, Aβ42, Aβ38, sAPPβ, sAPPα) and Aβ_{O} in healthy non-elderly subjects and AD patients. System and drug parameters were assumed to be the same for healthy subjects and AD patients, although this is a simplification of the likely non-homogeneous systems conditions during disease. An empirical drift model component was used to correct for the upward drift in CSF concentrations over the sampling period observed in healthy subjects (see Supplemental Material).

The model adequately predicted the response of Aβ40, Aβ42 and sAPPβ after a single dose in healthy volunteers (Figure 8.7 *left panels*). After 14 days of once-daily dosing of verubecestat in healthy volunteers, the response of Aβ40, Aβ42 and sAPPβ for the highest dose groups was slightly underpredicted (Figure 8.7 *middle panels*). In AD, the

model yielded a reasonable prediction of the observed biomarker response after 7 days of once-daily dosing (Figure 8.7 *right panels*).

The model predicted a decrease in the human $A\beta_O$ concentrations in CSF at the lumbar region (Figure 8.8 *middle row*). After a single 100 mg dose of verubecestat in healthy volunteers an 84% reduction in the predicted concentration of $A\beta_O$ was observed. This value is close to the 94% reduction at day 7 following repeated administration of once daily doses in the range of 40-150mg that was predicted by the model.

These simulations show that the translated model holds promise for use in the dose selection for clinical trials and to determine what dose level is needed to reach a predefined target % reduction in $A\beta_O$ concentrations. When clinical $A\beta_O$ concentration data from $A\beta$ production inhibitors would become available, the proposed model for the interspecies extrapolation could be verified.

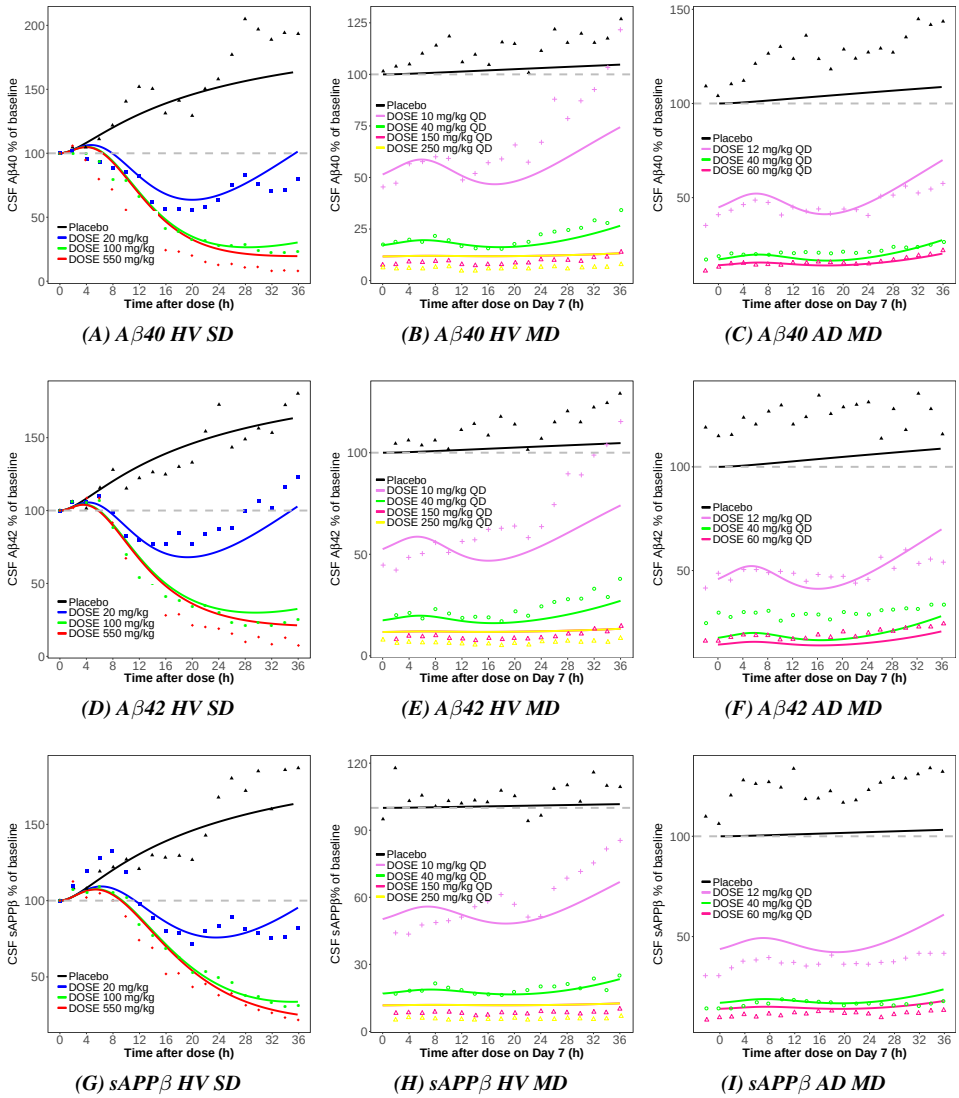

***Figure 8.7: Model based prediction of verubecestat effects on CSF Aβ40, Aβ42 and sAPPβ after a single dose (SD) in healthy volunteers (HV)* (left), *multiple dose (MD) in HV* (middle) *and MD in AD patients* (right).** Predictions are expressed as percentage relative to baseline. Symbols represent the median of observed percentage relative to baseline.

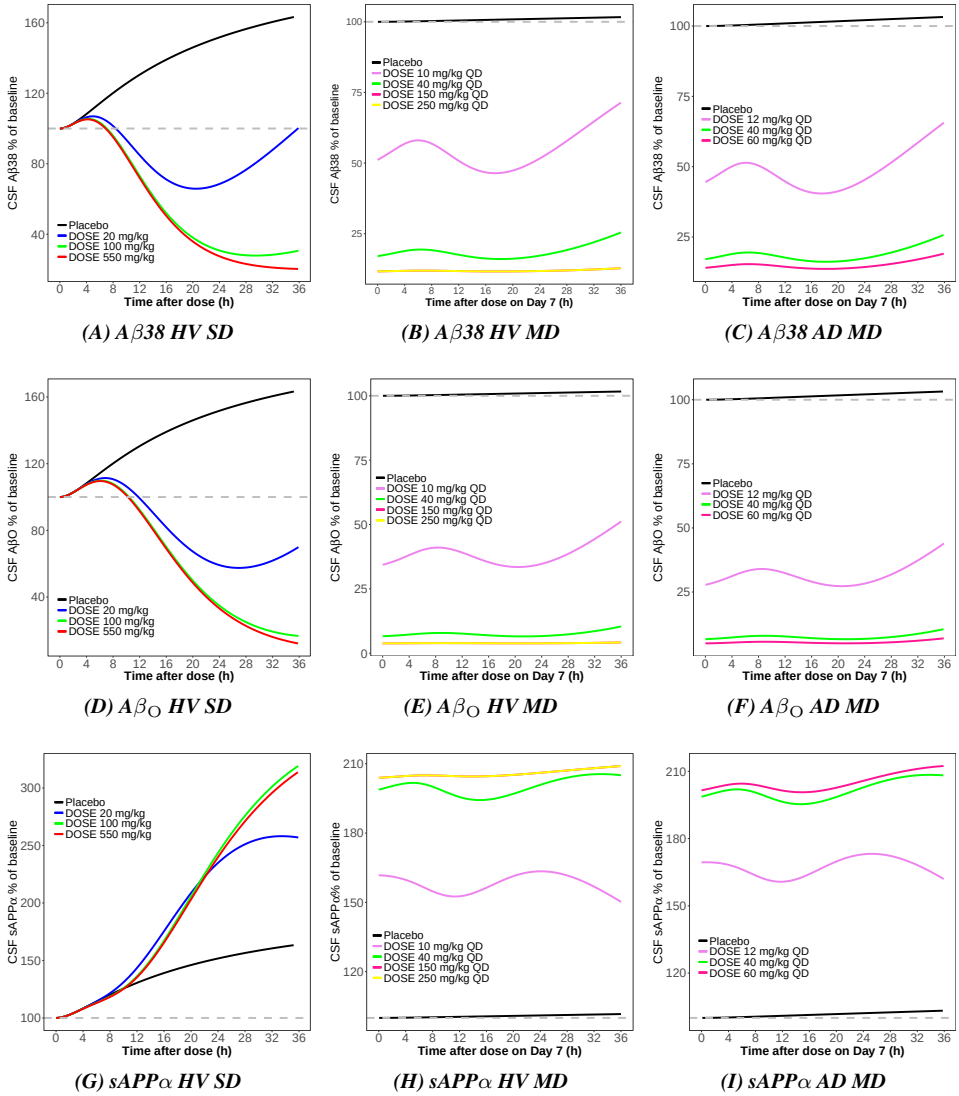

(A) Aβ38 HV SD ***(B) Aβ38 HV MD*** ***(C) Aβ38 AD MD***

(D) $A\beta_O$ HV SD ***(E) $A\beta_O$ HV MD*** ***(F) $A\beta_O$ AD MD***

(G) sAPPα HV SD ***(H) sAPPα HV MD*** ***(I) sAPPα AD MD***

***Figure 8.8: Model based prediction of verubecestat effects on CSF Aβ38, $A\beta_O$ and sAPPα after a single dose (SD) in healthy volunteers (HV)* (left)*, multiple dose (MD) in HV* (middle) *and MD in AD patients* (right).** Predictions are expressed as percentage relative to baseline. CSF Aβ38, $A\beta_O$ and sAPPα were not measured in these studies.

Perspectives in clinical studies in AD

The systems pharmacology model of the APP pathway in monkeys can be of value in the design and development of therapeutic interventions for AD in many ways. Here we briefly discuss a number of potentially useful applications.

Optimization of clinical study designs

Assessment of disease severity and treatment effect in clinical trials in AD constitutes a major challenge, due the lack of meaningful biomarkers reflecting disease severity, or predicting treatment effect. Moreover, frequently highly invasive techniques such as repeated sampling of CSF must be applied to obtain meaningful data. As a result, there is little room to optimize study protocols experimentally. Here we propose that modelling and simulation offers an informative approach to the optimization of the designs of clinical trials on the effects of novel drugs following single dose and repeated administration. This is exemplified in the optimization of the so-called SILK protocol. A number of years ago the protocol has been developed to determine kinetics of low-abundance proteins such as Aβ[14]. In this protocol, a primed bolus of $^{13}C_6$-Leucine is infused intravenously, at 2 mg/kg over 10 minutes, followed by 2 mg/kg/hours continuous infusion for 9 hours. The proportion of synthesized and secreted Aβ labelled with $^{13}C_6$-Leucine at amino acid 17 and 34 is measured, and the fraction of labelled Aβ in CSF is monitored for a number of hours after the end of the infusion[14]. As was mentioned earlier, the method has been successfully applied to assess differences in Aβ kinetics in cognitively normal persons versus symptomatic AD patients[15]. Recently, this SILK protocol has been used to assess the effect of drugs such as GS inhibitors on Aβ production[16]. Here, it is important to optimize the design of the SILK protocol, particularly in relation to the time of administration of the $^{13}C_6$-Leucine infusion relative to the time of administration of the drug and the interpretation of the signal.

Our studies on the effects of MBi-5 on the APP pathway in monkeys, using chemical assays (ELISA) for the quantification of the peptides showed a clear dose dependency for the effect on all APP metabolites (**Chapter 4**). However, in the same study such a dose dependency was not detected by the SILK protocol for the fraction labelled sAPPα. For sAPPβ and Aβ the sensitivity to detect dose proportionality appears to depend on, among other factors, the timing of administration of the $^{13}C_6$-Leucine infusion. An important question is how the design of the SILK protocol can be further optimized. Here, we use the β-13C-APP model to investigate in a series of simulations the effect of study design

features on the $^{13}C_6$-signal. These simulations focus specifically on i) the sensitivity to detect a treatment effect and ii) the possibility of identifying the exposure response relation. The details of the simulated scenarios are reported in the Supplemental Material.

These simulations showed that the timing of the $^{13}C_6$-Leucine infusion relative the drug dose and dose frequency affects the magnitude of the $^{13}C_6$-signal and the possibility to observe a dose proportionality in the signal. For the fraction labelled sAPPα signal, the protocol cannot be optimized further. This is caused by the fact that this APP metabolite is upstream of BACE1 inhibition. As a result of the inhibition of this enzyme unlabelled sAPPα accumulates, diluting the signal, independent of the timing of the $^{13}C_6$-Leucine infusion.

To investigate the effect of drugs, the SILK protocol should be optimized based on the best timing of the $^{13}C_6$-Leucine infusion for an endpoint which is closest to the target Aβ_O, which is fraction labelled Aβ. The optimal time of the $^{13}C_6$-leucine infusion depends on a number of factors, such as i) the PK of the drug under investigation, ii) the delay between the PK and BACE1 inhibition, iii) the delay between the kinetics of effects on Aβ relative to the kinetics of BACE1 inhibition and iv) the delay between start of $^{13}C_6$-Leucine infusion and sufficient enrichment at the target site. These factors can only be investigated simultaneously using an integrated model approach. Our simulations show that the greatest signal in terms of clear dose proportionality in fraction labelled Aβ is obtained when the $^{13}C_6$-Leucine infusion starts immediately after administration of the BACE1 inhibitor. The signal is already diminished when $^{13}C_6$-Leucine infusion starts at 1 hour post drug dose.

Early diagnosis

Initiating treatment early in the course of the disease is likely to be important when the aim is to slow or alter disease progression. The early diagnosis of preclinical AD is challenging, because patients do not display any symptoms presumably as result of a large resilience in the functioning of the biological system (**Chapter 2**). An important question is whether, and if so how, metabolites of the APP pathway might serve as biomarkers for the early detection of AD. It is well established that metabolite concentrations in CSF can reflect some of the pathophysiological changes that occur in the brain[17]. According to amyloid cascade hypothesis, the first step in the pathological cascade is accumulation of Aβ (Figure 2.3). CSF Aβ has therefore potential as a biomarker for (early) diagnosis and may provide clue of preclinical AD[18].

The development of biomarkers for the early detection of AD that are predictive of

preclinical AD constitutes a major challenge for a variety of reasons. First, the quantitation of metabolites of the APP pathway in CSF is technically difficult. As a result the reported values of CSF concentrations of Aβ can vary between different research centres and laboratories. This has led to a large initiative for the standardization of pre-analytical aspects of CSF biomarkers: The "Alzheimer's Association Cerebrospinal Fluid (CSF) Quality Control Program" brings together laboratories across the globe with the aim of standardizing the measurement of potential Alzheimer's biomarkers[19]. There has also been intensive research of aggregate-based biomarkers, including Aβ_{O} in CSF. However, to date, no biomarkers have been identified that can reliably diagnose AD in the early disease stage in an individual patient[20,21].

Second, due to the resilience in the biological system, changes in biomarkers may not be observed until advanced stages of the disease. An intriguing question is whether the sensitivity could be enhanced on the basis of a challenge test, analogous to the use of the glucose tolerance test for the detection of glucose intolerance as a precursor of type II diabetes mellitus[22]. For the APP pathway, the system could be challenged by the administration of a modulator such as a secretase inhibitor. The design of such a challenge test could be optimized on the basis of the systems pharmacology model of the APP network. Furthermore, the model-based analysis of the system response could yield estimates of system parameters that may serve as novel biomarkers which are indicative for the disease severity, and possibly predictive of the treatment response to APP modulating drugs.

Personalized treatment solutions

In most of the clinical trials in AD the molecular heterogeneity of the disease has not been taken into account. Because of such heterogeneity of AD, treatment may need to be stratified as, dependent on the genotype, response to potentially disease modifying therapeutics such as secretase inhibitors and Aβ clearance enhancers may be different.

In recent years important progress has been made in delineating genetic factors in the pathophysiology of AD related to changes in APP processing. Familial AD mutations in APP and in the presenilin genes PS-2 and PS-2 and at-risk gene polymorphisms responsible for late-onset AD all point to a unambiguous and early role of Aβ in the pathogenesis of AD[23,24,25]. In early-onset AD genetic variations were found on the APP gene as well as in the presenilin genes PS1 and PS2, encoding for the catalytic subunit of GS, causing altered APP processing[26,27,28]. In sporadic, late-onset AD the epsilon4 allele of the apolipoprotein E gene (APOE) was identified as a major risk factor contributing

to the pathogenesis of AD in about 20% of the cases[29,25]. Mechanistically, this can be understood by the fact that APOE is involved in the clearance and the aggregation of the Aβ peptide.

The current general thinking is that susceptibility for late-onset AD involves various genetic risk factors, as up to 60%-80% of the late-onset AD is genetically determined[27,30]. The genetic heterogeneity of the disease is high, and a large number of genetic risk factors, with relatively low penetrance but high prevalence must be involved. Also, genes with a modest contribution to the risk of AD may operate interactively[24]. A few risk factors, supporting the amyloid hypothesis, are discussed in the Supplemental Material. It is important that genetic information is considered in future clinical trials with drugs acting at the APP pathway.

The genetic information may be utilized in various ways. Firstly, this may hint to system parameters that need to be adjusted to describe the disease state. Secondly, an individual's genetic susceptibility may serve as a preselection criterion for further diagnostic tests as well as personalized treatment of interventions targeting the APP pathway.

Prediction of the long term treatment effect

Future treatments for AD are likely to be interventions that modify the progression of the disease[17]. Demonstration of a drug effect on disease progression is notoriously difficult due to the slow progression of the disease and the typically wide inter-individual variation in the rate of progression. An additional complicating factor is that the statistical techniques that are applied in the evaluation of clinical trials (such as analysis of variance) are not valid in the case of a chronically progressive disease. Moreover, they do not differentiate between symptomatic and disease modifying effects. To meet these challenges, the concept of disease progression analysis has been introduced[31,32]. Disease progression analysis utilizes regression models to estimate the rate of disease progression. Using a simple linear regression model and the Alzheimer Disease Assessment Scale – Cognition subscale (ADAS-Cog) score as a pharmacodynamic endpoint it was found that AD progresses at a rate of 8.2 units per year[33].

It remains to be determined however whether disease severity progresses linearly with time. Here it is of interest that the rate of progression was slower at earlier stages of the disease[34]. Moreover, the ADAS-Cog score can only be used as a disease status marker when cognitive changes have commenced. Therefore, in the early phases of the disease and for the design of pre-emptive studies other biomarkers and a more complex disease

progression model are needed. To overcome these and other complexities, the concept of disease systems analysis has been introduced as a mechanistic alternative to disease progression analysis Post et al. [35].

In "disease systems analysis" the disease progression is modelled on the basis of a cascade of turnover models to describe the biomarker responses. This opens the possibility to connect changes in biomarker responses at the early stages of the disease to changes in behavioural endpoints (i.e. rating scales such as the ADAS-Cog score) at later stages. The systems pharmacology models that have been introduced in this thesis are based on the same concept of cascading turnover models and constitute therefore a basis for disease systems analysis models in AD. These models can be extended to comprise also the effects on further downstream biomarkers. The next biomarker to become abnormal is amyloid-PET, reflecting accumulation of cortical Aβ fibrils, followed by CSF tau, indicative for neurofibrillary tangles (NFT), followed by biomarkers for neurodegeneration (fluorodeoxyglucose [FDG]-PET and structural magnetic resonance imaging [MRI]). Cognitive impairment is the last event in the progression of the disease (2.3). New biomarkers to measure disease progression in AD may became available over the years.

To integrate these biomarkers in a disease systems model, the correlations between these biomarkers need to be considered, firstly, between the biochemical markers CSF Aβ and tau, secondly between fluid and imaging biomarkers, and ultimately with ADAS-Cog scores. Most of these correlations are investigated in clinical-autopsy correlation studies. In order to be able to capture disease progression longitudinal data in the same subjects are needed. However, this type of data in the same subjects is rare and new initiatives are needed in this respect. One of the first initiatives currently ongoing is the 'Alzheimer's Disease Neuroimaging Initiative' (ADNI). The ADNI is studying the rate of cognition decline, change is brain structures and fluid biomarkers among volunteers over 55 years, who are healthy, as well as those who have been diagnosed with mild dementia due to AD.

Alternative interventions targeting the APP pathway

We have developed a systems pharmacology model of the APP pathway on the basis of Aβ production inhibitors (BACE1 and GS inhibition) and quantified their effects on Aβ_{O}. In theory, to reduce Aβ burden the functioning of the APP pathway can be modified in many different ways: (1) inhibition of Aβ production; (2) enhancement of Aβ clearance;

(3) blocking Aβ_O toxicity through interactions with the Aβ_O target site.

Until now, clinical trials of Aβ production inhibitors (i.e. BACE1 and GS inhibitors) could not demonstrate clinical efficacy at tolerated doses in patients[36,37,38]. Moreover, the anti-Aβ monoclonal antibodies, developed to enhance Aβ clearance, bapineuzumab (Pfizer Inc.) and solanezumab (Eli Lilly & Co.) could not demonstrate efficacy in AD patients large Phase III clinical trials[39,40]. In general, for amyloid-targeted therapy there is now a tendency to move towards clinical trials with prodromal AD or in subjects at preclinical stage of familial hereditary AD variants.

The primary endpoints for efficacy in the clinical AD studies were measures of cognitive performance by changes in ADAS-Cog score and in the AD Cooperative Study – Activities of Daily Living (ADCS-ADL) score. There are several possible explanations for the lack of efficacy. A particularly important question is whether target engagement as reflected in the exposure to Aβ_O has been achieved. The β-γ-O-APP model could be used to predict this.

In this section, the β-γ-O-APP model is used to perform simulations to investigate interventions targeting the APP pathway. The behaviour of the individual moieties of the β-γ-O-APP model was evaluated by simulating the responses after Aβ production inhibition (BACE1 or GS inhibition) and by triggering the system with a hypothetical compound enhancing Aβ clearance (Figure 8.9). The hypothetical Aβ clearance enhancer was assumed to have similar PK properties as the BACE1 inhibitor. An Emax concentration effect relationship was simulated assuming a maximal increase of the Aβ clearance rate constant (Kout) by 5 fold.The simulation showed that the effect of the Aβ clearance enhancer yielded less reduction in Aβ_O concentration (83.4%) than production inhibition (86.8% and 87.4% for BACE1 and GS inhibitor, respectively). Furthermore, Aβ clearance enhancement does not affect APP, sAPPβ, C99 and sAPPα concentrations.

The β-γ-O-APP model offers the opportunity to investigate the net system's responses to combined intervention acting at different targets. Therefore, the system was triggered by combined administration of two compounds: a combination of a BACE1 and GS inhibitor, a combination of a GS inhibitor and Aβ clearance enhancer and a combination of a BACE1 inhibitor and Aβ clearance enhancer (Figure 8.10). The effects of the different treatments were assumed to be additive and no PK interactions were taken into consideration.

Combined administration of MBi-5 and MK-0752 would further reduce Aβ monomers and Aβ_O concentrations compared to monotherapy: a reduction of 97% in Aβ_O was achieved with combined administration. Combining two drugs with similar action (Aβ production inhibition), provided less reduction in Aβ_O concentrations than a combination

of GS inhibition and Aβ clearance enhancement (98.5%), although differences are small. These simulations showed an additive response on Aβ_{O} concentrations of combined intervention. Further pharmacodynamic drug interaction studies may be required to investigate a possible synergistic effect, in which response surface analysis may be used to elucidate the drug interactions fully[41].

A promising strategy seems to be the prevention of toxicological effects by preventing the interaction of toxic Aβ_{O} species with target receptors. Such novel therapies pharmacologically compete with Aβ_{O} with critical receptor targets, thereby preventing synapse loss and improving memory. An example of such receptor targets are the sigma-2/PGRMC1 receptors that mediate Aβ_{O} binding to the synaptic puncta on neurons[42]. One such candidate compound targeting these receptors is the small molecule therapeutic CT1812 (Cognition Therapeutics, Inc.), which is in clinical testing in AD patients. Adding information from CT1812 study data would provide the opportunity to extend the β-γ-O-APP model with a receptor interaction model component for Aβ_{O}-receptor interactions. Then, it would be of interest to investigate what happens to the Aβ equilibrium when Aβ_{O} concentrations rise as result of receptor blockage. The increase of Aβ_{O} in the brain may lead to redistribution of Aβ_{O} into the CSF and more effective elimination. Or it could lead to the undesirable effect of increased fibril formation. In that respect, extension of the model to describe the higher ordered agglomerated species as fibrils and plaques would be essential. For an effective suppression of the Aβ_{O} concentrations and it's toxic effects if probably necessary to use rational combinations of drugs targeting multiple targets in the system. Once the β-γ-O-APP model is extended, the combined intervention of an Aβ production inhibitor and prevention of the interaction of Aβ_{O} species with it's receptor target can be investigated such that therapy may be optimized.

The APP systems pharmacology model can bring us closer to optimizing the therapeutic intervention to reduce oligomer burden in AD. This thesis shows that systems pharmacology models provide a powerful tool for integrated analysis of biology and pharmacology to assess system-drug interactions that is difficult to study in other ways. Further, the model constitutes the basis for the development of a disease systems model for AD to investigate the effect of disease modifying treatments on disease progression. Because of a common pathological principle, this approach can also be applied to other protein misfolding neurodegenerative disease such as PD, HD and ALS. An ultimate objective would be to combine disease system models to investigate common pathological paths as well as disease-specific signatures in protein misfolding neurodegenerative diseases.

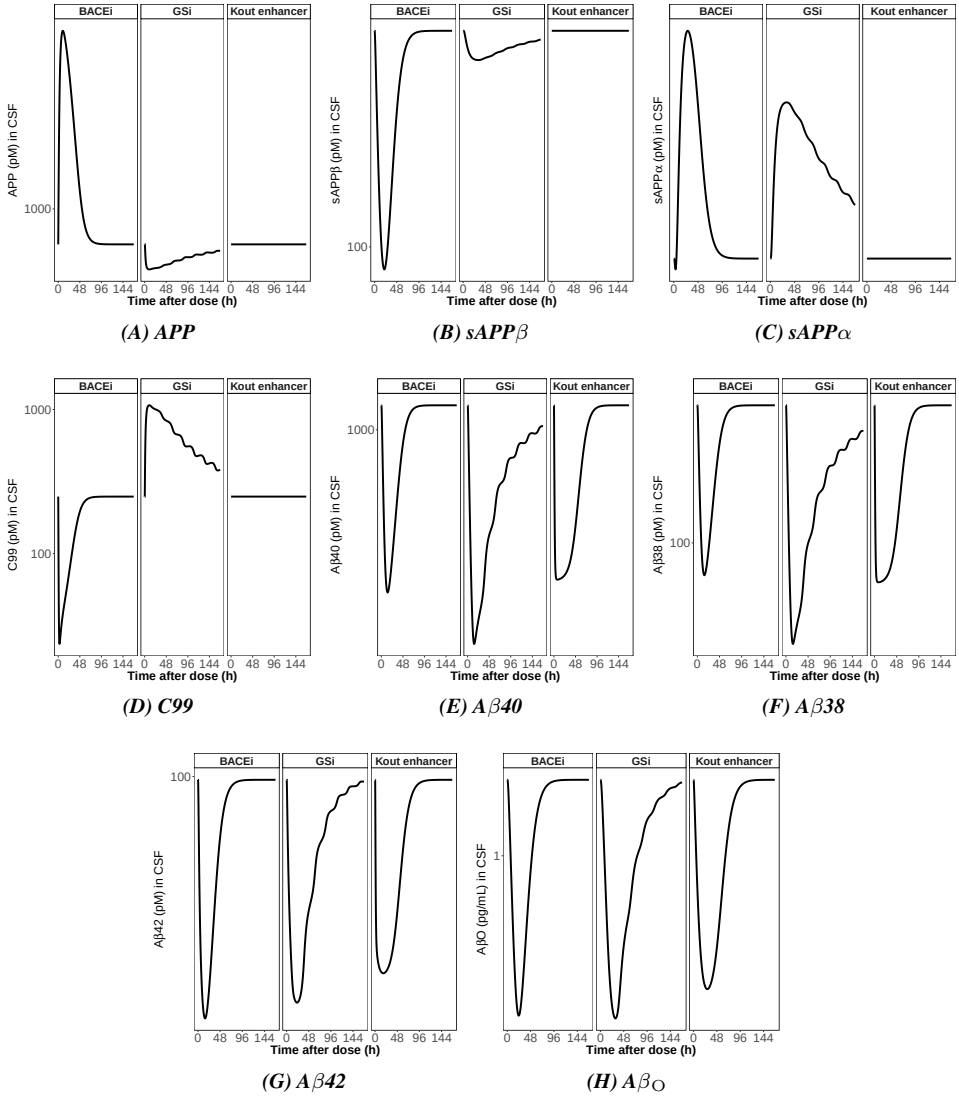

(A) APP *(B) sAPPβ* *(C) sAPPα*

(D) C99 *(E) Aβ40* *(F) Aβ38*

(G) Aβ42 *(H) Aβ_{O}*

***Figure 8.9: Different moieties of β-γ-O-APP model in response to 125 mg/kg MBi-5* (left panels)*, 240 mg/kg MK-0752* (middle panels) *and hypothetical compound (Aβ clearance enhancer)* (right panels).**

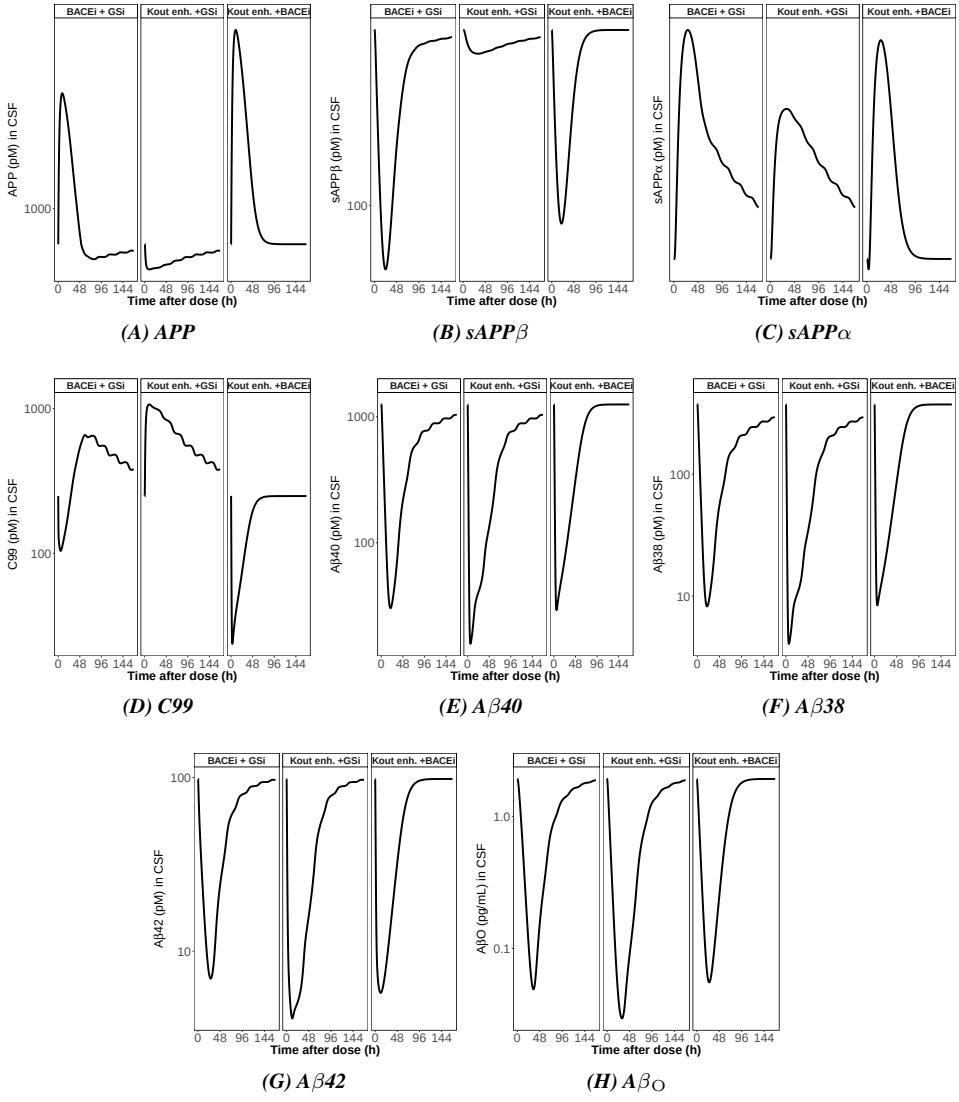

(A) APP ***(B) sAPPβ*** ***(C) sAPPα***

(D) C99 ***(E) Aβ40*** ***(F) Aβ38***

(G) Aβ42 ***(H) Aβ_{O}***

Figure 8.10: Different moieties of β-γ-O-APP model in response to combination of 125 mg/kg MBi-5 and 240 mg/kg MK-0752* (left panels)*, the combination of 240 mg/kg MK-0752 and hypothetical compound (Aβ clearance enhancer)* (middle panels) *and the combination of 125 mg/kg MBi-5 and hypothetical compound (Aβ clearance enhancer)* (right panels)*.

References

1. Gilberto, D.B., *et al.* An alternative method of chronic cerebrospinal fluid collection via the cisterna magna in conscious rhesus monkeys. Contemp Top Lab Anim Sci. 2003;42 (4):53–59.
2. Ogata, Y., Charlesworth, M.C., & Muddiman, D.C. Evaluation of protein depletion methods for the analysis of total-, phospho- and glycoproteins in lumbar cerebrospinal fluid. J Proteome Res. 2005;4(3):837–845.
3. Mikkonen, S., Jacksen, J., Roeraade, J., Thormann, W., & Emmer, A. Microfluidic Isoelectric Focusing of Amyloid Beta Peptides Followed by Micropillar-Matrix-Assisted Laser Desorption Ionization-Mass Spectrometry. Anal Chem. 2016;88(20): 10044–10051.
4. Savage, M.J., *et al.* A sensitive Aβ oligomer assay discriminates Alzheimer's and aged control cerebrospinal fluid. J Neurosci. 2014;34(8):2884–97.
5. Podlisny, M.B., Tolan, D.R., & Selkoe, D.J. Homology of the amyloid beta protein precursor in monkey and human supports a primate model for beta amyloidosis in Alzheimer's disease. Am J Pathol. 1991;138 (6):1423–1435.
6. Heuer, E., Rosen, R.F., Cintron, A., & Walker, L.C. Nonhuman primate models of Alzheimer-like cerebral proteopathy. Curr Pharm Des. 2012;18(8):1159–1169.
7. Franco, R., Navarro, G., E, M.P., & Moreno, E. Amyloid Beta Precursor Protein: Proper Credit for the Basic Biochemical Properties of the Most Studied Protein in the 21st Century*. J Neurol Neurol Disord. 2014;1(1): 1–6.
8. Rosen, R.F., Walker, L.C., & Iii, H.L. PIB binding in aged primate brain: Enrichment of high-affinity sites in humans with Alzheimer's disease 2012;32(2):223–234.
9. Mager, D.E., Woo, S., & Jusko, W.J. Scaling Pharmacodynamics from In Vitro and Preclinical Animal Studies to Humans. Drug Metab Pharmacokinet. 2009;24(1):16–24.
10. Stevens, J., *et al.* Mechanism-based PK-PD model for the prolactin biological system response following an acute dopamine inhibition challenge: quantitative extrapolation to humans. J Pharmacokinet Pharmacodyn. 2012;39(5):463–77.
11. Kleijn, H.J., *et al.* Development and Application of a Semi-Mechanistic Model for Modulation of Amyloid-β in Cerebrospinal Fluid after Inhibition of γ-secretase. Poster Present PAGE, Athens, Greece. 2011.
12. Kennedy, M.E., *et al.* The BACE1 inhibitor verubecestat (MK-8931) reduces CNS β-amyloid in animal models and in Alzheimers disease patients. Sci Transl Med. 2016;8(363):363ra150–363ra150.
13. Ma, L., *et al.* Population pharmacokinetic modeling of the novel BACE inhibitor MK-8931 following single and multiple dose administration in healthy subjects. Poster Sess Present AAIC. 2012;pages P1–229.
14. Bateman, R.J., Munsell, L.Y., Chen, X., Holtzman, D.M., & Yarasheski, K.E. Stable

isotope labeling tandem mass spectrometry (SILT) to quantify protein production and clearance rates. J Am Soc Mass Spectrom. 2007;18(6):997–1006.

15. Mawuenyega, K.G., *et al.* Decreased clearance of CNS beta-amyloid in Alzheimer's disease.. Science. 2010;330(6012):1774.
16. Bateman, R.J., *et al.* A gamma-secretase inhibitor decreases amyloid-beta production in the central nervous system. Ann Neurol. 2010;66(1):48–54.
17. Lleó, A., *et al.* Cerebrospinal fluid biomarkers in trials for Alzheimer and Parkinson diseases. Nat Rev Neurol. 2015;11:41–55.
18. Anoop, A., Singh, P.K., Jacob, R.S., & Maji, S.K. CSF Biomarkers for Alzheimer's Disease Diagnosis.. Int J Alzheimers Dis. 2010;2010(Table 1):1–12.
19. Mattsson, N., Andreasson, U., & Persson, S. The Alzheimer's Association external quality control program for cerebrospinal fluid biomarkers. NIH Public Access. 2013;7(4): 386–395.
20. Giacomelli, C., Daniele, S., & Martini, C. Potential biomarkers and novel pharmacological targets in protein aggregation-related neurodegenerative diseases. Biochem Pharmacol. 2017;131:1–15.
21. Hölttä, M., *et al.* Evaluating amyloid-β oligomers in cerebrospinal fluid as a biomarker for Alzheimer's disease.. PLoS One. 2013;8(6):e66381.
22. Unwin, N., Shaw, J., Zimmet, P., & Alberti, K.G. Impaired glucose tolerance and impaired fasting glycaemia: The current status on definition and intervention. Diabet Med. 2002;19(9):708–723.
23. Bilousova, T., *et al.* Synaptic Amyloid-β Oligomers Precede p-Tau and Differentiate High Pathology Control Cases. Am J Pathol. 2016;186(1):185–198.
24. Campion, D., Pottier, C., Nicolas, G., Le Guennec, K., & Rovelet-Lecrux, A. Alzheimer disease: modeling an Aβ-centered biological network. Mol Psychiatry. 2016;21(7):861–871.
25. Nicolas, G., Charbonnier, C., & Campion, D. From common to rare variants: The genetic component of Alzheimer disease. Hum Hered. 2017;81(3):129–141.
26. Chávez-Gutiérrez, L., *et al.* The mechanism of γ-Secretase dysfunction in familial Alzheimer disease. EMBO J. 2012;31(10): 2261–74.
27. Bertram, L., Lill, C.M., & Tanzi, R.E. The genetics of alzheimer disease: Back to the future. Neuron. 2010;68(2):270–281.
28. Veugelen, S., Saito, T., Saido, T.C., Chávez-Gutiérrez, L., & De Strooper, B. Familial Alzheimer's Disease Mutations in Presenilin Generate Amyloidogenic Aβ Peptide Seeds. Neuron. 2016;90(2):410–416.
29. Bertram, L., McQueen, M.B., Mullin, K., Blacker, D., & Tanzi, R.E. Systematic meta-analyses of Alzheimer disease genetic association studies: the AlzGene database. Nat Genet. 2007;39(1):17–23.
30. Gatz, M., *et al.* Role of genes and environments for explaining Alzheimer disease.. Arch Gen Psychiatry. 2006;63(2):168–174.
31. Holford, N. Disease progression and neuroscience. J Pharmacokinet Pharmacodyn. 2013;40(3):369–376.

32. Holford, N. Clinical pharmacology = disease progression + drug action. Br J Clin Pharmacol. 2015;79(1):18–27.

33. Yesavage, J.A., Poulsen, S.L., Sheikh, J., & Tanke, E. Rates of change of common measures of impairment in senile dementia of the Alzheimer's type. Psychopharmacol.Bull.. 1988;24(0048-5764):531–534.

34. Samtani, M.N., *et al.* An improved model for disease progression in patients from the Alzheimer's disease neuroimaging initiative.. J Clin Pharmacol. 2012;52(5):629–44.

35. Post, T.M., Freijer, J.I., DeJongh, J., & Danhof, M. Disease system analysis: Basic disease progression models in degenerative disease. Pharm Res. 2005;22(7):1038–1049.

36. Toyn, J. What lessons can be learned from failed Alzheimer's disease trials? Expert Rev Clin Pharmacol. 2015;8(3):1–3.

37. Kennedy, M.E., *et al.* The BACE1 inhibitor verubecestat (MK-8931) reduces CNS β-amyloid in animal models and in Alzheimers disease patients. Sci Transl Med. 2016;8(363):363ra150–363ra150.

38. Hawkes, N. Merck ends trial of potential Alzheimer's drug verubecestat. Bmj. 2017;845:j845.

39. Panza, F., Logroscino, G., Imbimbo, B.P., & Solfrizzi, V. Is there still any hope for amyloid-based immunotherapy for Alzheimer's disease? Curr Opin Psychiatry. 2014;27(2):128–137.

40. Panza, F., *et al.* Emerging drugs to reduce abnormal β-amyloid protein in Alzheimer's disease patients. Expert Opin Emerg Drugs. 2016;21(4):377–391.

41. Jonker, D.M., Visser, S.A., Van Der Graaf, P.H., Voskuyl, R.A., & Danhof, M. Towards a mechanism-based analysis of pharmacodynamic drug-drug interactions in vivo. Pharmacol Ther. 2005;106(1):1–18.

42. Izzo, N.J., *et al.* Alzheimer's therapeutics targeting amyloid beta 1-42 oligomers I: Abeta 42 oligomer binding to specific neuronal receptors is displaced by drug candidates that improve cognitive deficits. PLoS One. 2014;9(11):27–29.

Chapter 8

Supplemental Material

Supplement to

Systems pharmacology of the amyloid precursor protein pathway in Alzheimer's disease
- Conclusions & perspectives

SUPPLEMENTAL MATERIAL

Perspectives in clinical studies in AD - Drift behaviour

In the reported human studies on verubecestat[1], observed lumbar CSF concentrations increased over the sampling period of 36 hours (Figure S8.1). It may be related to the transport to the lumbar region or an artefact of repeated sampling from lumbar region[2] and on the volume removed relative to the total CSF in spine. This drift behaviour is subjected to between-study variation, as result of differences in study procedures and how the lumbar samples were drawn. If this drift is not accounted for in the model, the drug effect may be underpredicted. Therefore, the drift was predicted by an empirical drift model component, similar to the drift model reported by Kleijn et al.[3].

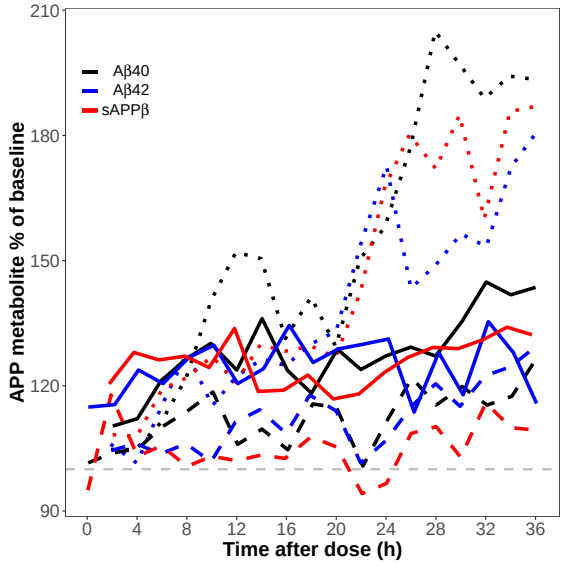

Figure S8.1: Comparison observed CSF concentrations of Aβ40* (black*), Aβ42* (blue*), and sAPPβ* (red*) after last placebo administration over the 36-hour sampling period for healthy volunteers after single dose* (dashed line*), once-daily doses for 14 days* (long-dashed line*) and for AD patients after once-daily doses for 7 days* (solid line*).

Optimization of clinical study designs - Simulation scenarios

The β-13C-APP model was used to investigate the effect of study design features on the 13C signal (Chapter 8). The simulated scenarios are presented in Table S8.1.

Table S8.1: Simulation scenarios

Scenario	Investigation objective	MBi-5 dose (mg/kg)	$^{13}C_6$-Leu administration timing[a]	Figure
A	Effect of time of administration of $^{13}C_6$-Leu primed infusion relative to the time of administration of MBi-5	125 single dose (SD)	0, 2, 4, 6, 8, 10 or 12 h post SD	S8.2
B	Effect on the dose proportionality of MBi-5 with $^{13}C_6$-Leu primed infusion at various time points following the administration of MBi-5	SD 1, 5, 10, 30, 60, 90, 125	1, 6 or 12 h post SD	S8.3
C	Effect on $^{13}C_6$-signal upon repeated dosing of MBi-5	0, 10, 30, 125 once daily (OD) for 5 days	1 h post last dose	S8.4
D	Effect on the dose proportionality in the $^{13}C_6$-signal upon repeated dosing of a dose range of MBi-5 OD with $^{13}C_6$-Leu primed infusions started 1 h after drug dose on various days	0, 10, 30, 125 mg/kg OD for 5 days	1 h after drug dose on day 1, 2, 3, 4 or 5	S8.5

[a] relative to MBi-5 dose

Optimization of clinical study designs- Simulation results

Simulation on scenario A showed that the timing of $^{13}C_6$-Leu primed infusion has an influence on the magnitude of the $^{13}C_6$-signal as reflected in the fraction labelled Aβ, fraction labelled sAPPα and fraction labelled sAPPβ (Figure S8.2). For fraction labelled Aβ and fraction labelled sAPPβ the highest signal was obtained when starting the infusion 12 hours post drug dose, whereas for fraction labelled sAPPα the signal is maximal when the infusion starts at the same time as drug dose.

Simulations of scenario B indicated that for the low MBi-5 dose levels (<30 mg/kg), increase of $^{13}C_6$-Leucine infusion start time relative to the administration of the drug results in a loss of dose proportionality. For sAPPα dose proportionality was not evident at 1 hour post drug and this was worsened at 6 and 12 hours post drug. For sAPPβ, the dose proportionality of the $^{13}C_6$-signal diminished with increasing $^{13}C_6$-Leucine infusion post drug start time, in particular after low MBi-5 doses (<30 mg/kg) (Figure S8.3).

Simulations of scenario C showed that the dose dependency in the $^{13}C_6$-signal was absent after once daily administration of MBi-5 during 5 days, while a dose dependent response was predicted in the absolute protein concentrations (Figure S8.4).

Scenario D illustrated that the $^{13}C_6$-signal in fraction labelled Aβ diminished with time when dosed once daily (Figure S8.5).

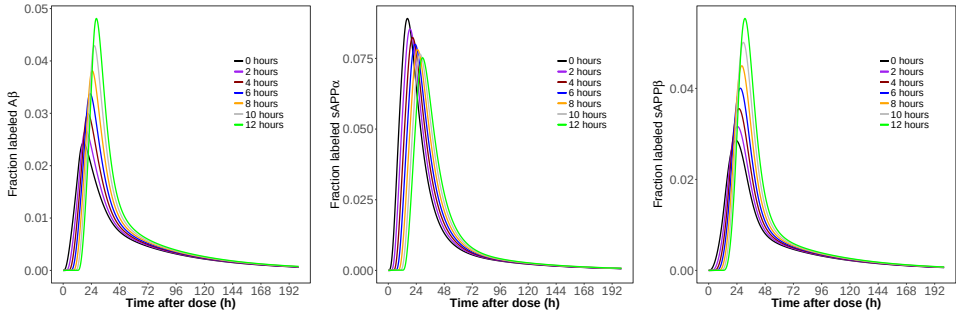

(A) Fraction labeled Aβ ***(B) Fraction labeled sAPPα*** ***(C) Fraction labeled sAPPβ***

Figure S8.2: Simulation tracer kinetic profiles (fraction labeled Aβ (A), fraction labeled sAPPα (B), fraction labeled sAPPβ (C)) with the β-13C-APP model.
Simulation scenario A: The start time of the $^{13}C_6$-Leucine infusion relative to the MBi-5 administration (125 mg/kg dose) is varied from 0 up to 12 hours post drug.

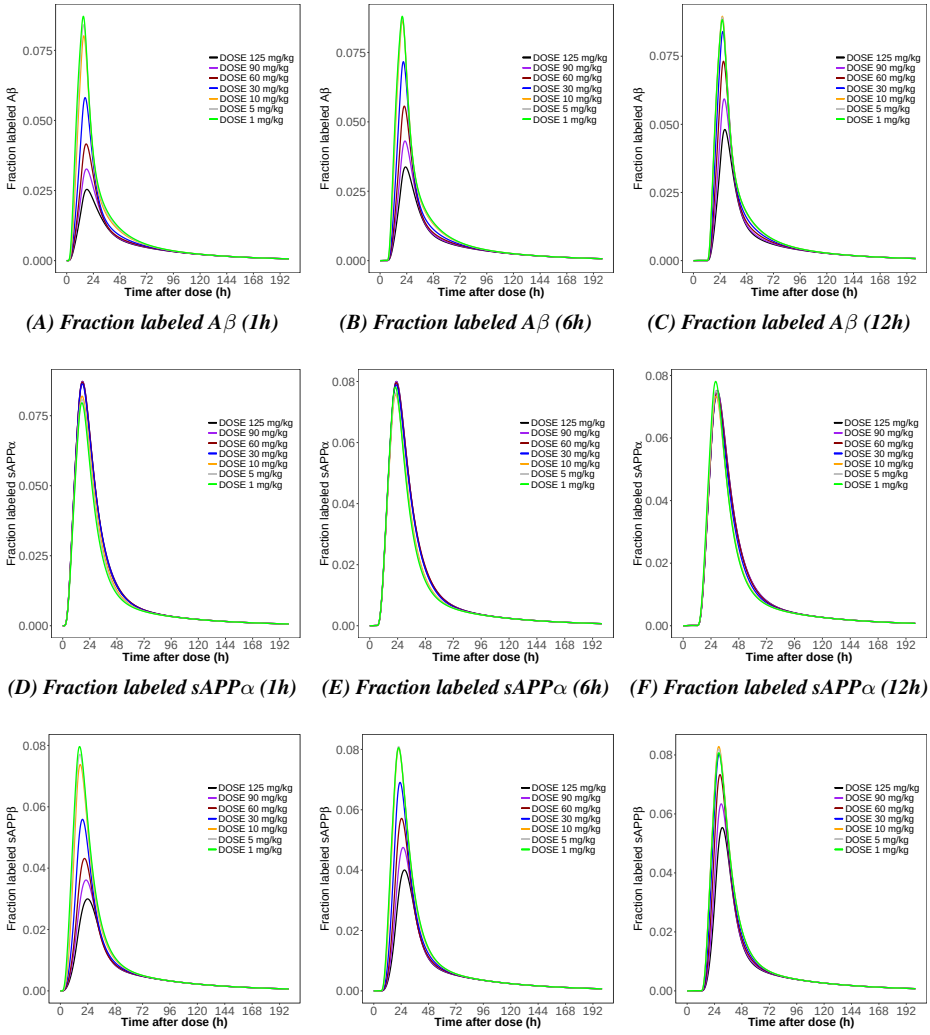

(A) Fraction labeled Aβ (1h) ***(B) Fraction labeled Aβ (6h)*** ***(C) Fraction labeled Aβ (12h)***

(D) Fraction labeled sAPPα (1h) ***(E) Fraction labeled sAPPα (6h)*** ***(F) Fraction labeled sAPPα (12h)***

(G) Fraction labeled sAPPβ (1h) ***(H) Fraction labeled sAPPβ (6h)*** ***(I) Fraction labeled sAPPβ (12h)***

Figure S8.3: Simulation tracer kinetic profiles with the β-13C-APP model.
Simulation scenario B: The start time of the $^{13}C_6$-Leucine infusion relative to the MBi-5 administration is varied (1, 6 and 12 hours post drug) and a dose range of MBi-5 (1 up to 125 mg/kg) is simulated.
Top panels: fraction labeled Aβ; *Middle panels:* fraction labeled sAPPα; *Bottom panels:* fraction labeled sAPPβ.

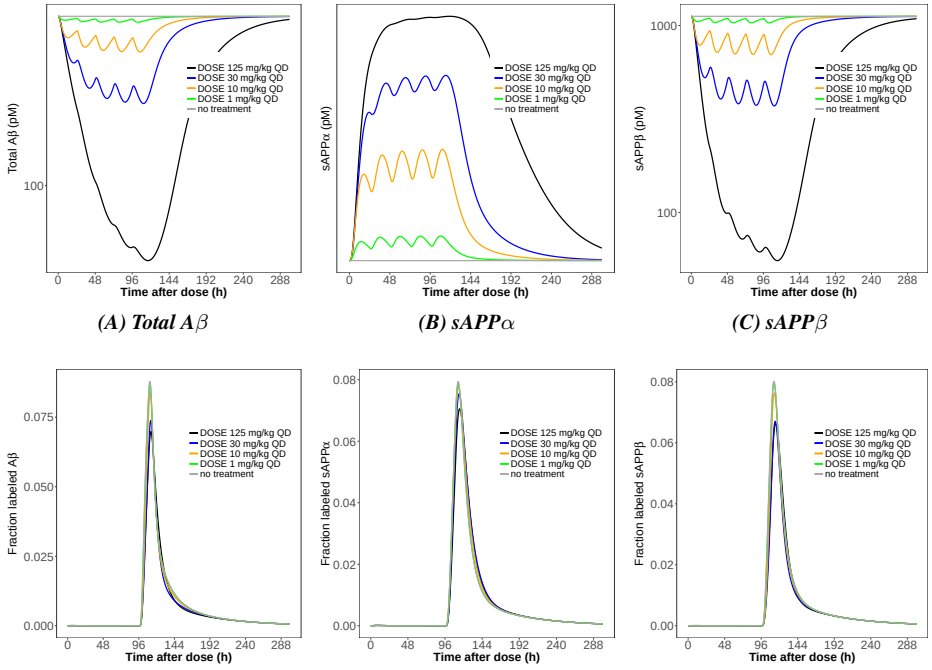

Figure S8.4: Simulation absolute protein concentrations and tracer kinetic profiles of APP metabolites with the β-13C-APP model.

Simulation scenario C: Once daily dosing MBi-5 for 5 days, varying MBi-5 dose (0, 10, 30, 125 mg/kg). The start time of the $^{13}C_6$-Leucine infusion relative to the MBi-5 administration is fixed to 1h after last dose.

Top panels: Absolute protein concentrations; *Bottom panels:* tracer kinetic profiles.

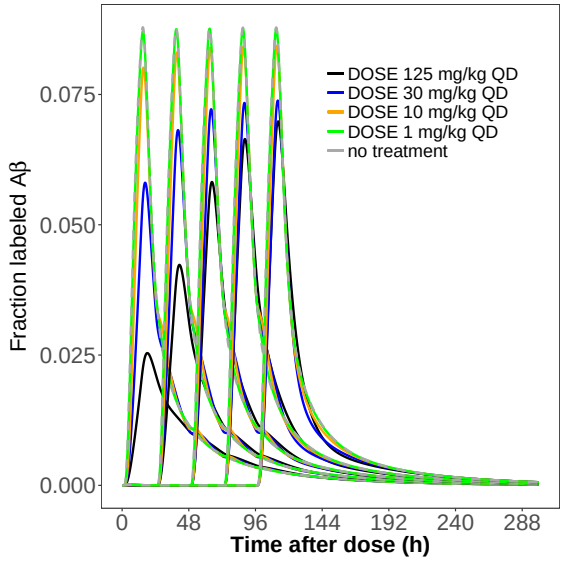

Figure S8.5: Simulation tracer kinetic profiles of Aβ with the β-13C-APP model.
Simulation scenario D: Once daily dosing MBi-5 for 5 days, varying MBi-5 dose (0, 10, 30, 125 mg/kg). The start time of the $^{13}C_6$-Leucine infusion relative to the MBi-5 administration is 1 hour after MBi-5 dose on day 1, 2, 3, 4 and 5.

Personalized treatment solutions- Examples of genetic risk factors

The Triggering Receptor Expressed On Myeloid Cells 2 (TREM2) variant p.R47H and p.A673T APP variant have been associated with AD risk or protection. TREM2 is expresses on microglial cells and has a role in regulating the response of the innate immune system to Aβ pathology and facilitating Aβ phagocytosis[4]. It binds to anionic lipids that interact with Aβ fibrils and apoliproteins, such as APOE. The p.R47H TREM2 variant weakens microglial detection of these lipids, thereby decreasing Aβ clearance. The APP p.A673T variant is close to the BACE1 cleavage site, making APP a less favourable substrate for the β-cleavage path[5].

Association analyses at the gene level have revealed that the loss-of-function in the sortilin related receptor 1 (SORL1) and ATP-binding cassette transporter A7 (Aβ CA7) genes are a moderate risk factor of AD. The SORL1 encodes a cargo protein which can bind APP and direct its processing to non-amyloidogenic pathways. It can also bind Aβ peptide and direct it to the lysosome, leading to its degradation[6]. Loss-of-function

of SORL1 has been linked with increased late onset AD risk[5]. Several rare variants in Aβ CA7 have been identified as risk factors of late onset AD, although its precise role in AD pathogenesis is not well understood. Aβ CA7 is primarily expressed in microglial cells and has a lipid transport function. It may be involved in Aβ clearance or production as Aβ CA7 knockout mice showed an increase in amyloid plaques[6,5,7].

References

1. Kennedy, M.E., *et al.* The BACE1 inhibitor verubecestat (MK-8931) reduces CNS β-amyloid in animal models and in Alzheimers disease patients. Sci Transl Med. 2016;8 (363):363ra150–363ra150.

2. Lucey, B.P., *et al.* An integrated multi-study analysis of intra-subject variability in cerebrospinal fluid amyloid-β concentrations collected by lumbar puncture and indwelling lumbar catheter. Alzheimers Res Ther. 2015;7(1):53.

3. Kleijn, H.J., *et al.* Development and Application of a Semi-Mechanistic Model for Modulation of Amyloid-β in Cerebrospinal Fluid after Inhibition of γ-secretase. Poster Present PAGE, Athens, Greece. 2011.

4. Ulrich, J.D., Ulland, T.K., Colonna, M., & Holtzman, D.M. Elucidating the Role of TREM2 in Alzheimer's Disease. Neuron. 2017;94(2):237–248.

5. Nicolas, G., Charbonnier, C., & Campion, D. From common to rare variants: The genetic component of Alzheimer disease. Hum Hered. 2017;81(3):129–141.

6. Campion, D., Pottier, C., Nicolas, G., Le Guennec, K., & Rovelet-Lecrux, A. Alzheimer disease: modeling an Aβ-centered biological network. Mol Psychiatry. 2016;21 (7):861–871.

7. Kunkle, B.W., *et al.* Targeted sequencing of ABCA7 identifies splicing, stop-gain and intronic risk variants for Alzheimer disease. Neurosci Lett. 2017;649:124–129.